

Supporting Information

Synthesis, Radiosynthesis, and Biological Evaluation of Carbon-11 Labeled 2β -Carbomethoxy- 3β -(3'-((Z)-2-haloethyl)phenyl)nortropanes: Candidate Radioligands for *In Vivo* Imaging of the Serotonin Transporter with Positron Emission Tomography

Jeffrey S. Stehouwer,[†] Nachwa Jarkas,[†] Fanxing Zeng,[†] Ronald J. Voll,[†] Larry Williams,[†] Michael J. Owens,[§] John R. Votaw,[†] and Mark M. Goodman*^{†§}

Department of Radiology, Department of Psychiatry and Behavioral Sciences, Emory University, 1364 Clifton Road NE, Atlanta, GA 30322

[†] Department of Radiology

[§] Department of Psychiatry and Behavioral Sciences

Table of Contents

MicroPET Time-Activity Curves and Uptake Data	S2-S4
Discussion of purity of 1 and 2 used for binding assays	S5
¹ H NMR spectra of 1 and 2 used for binding assays	S6
X-ray crystal structure of 1 and crystal packing description	S7-S9
Crystallography experimental and data tables	S10-S18

MicroPET Imaging

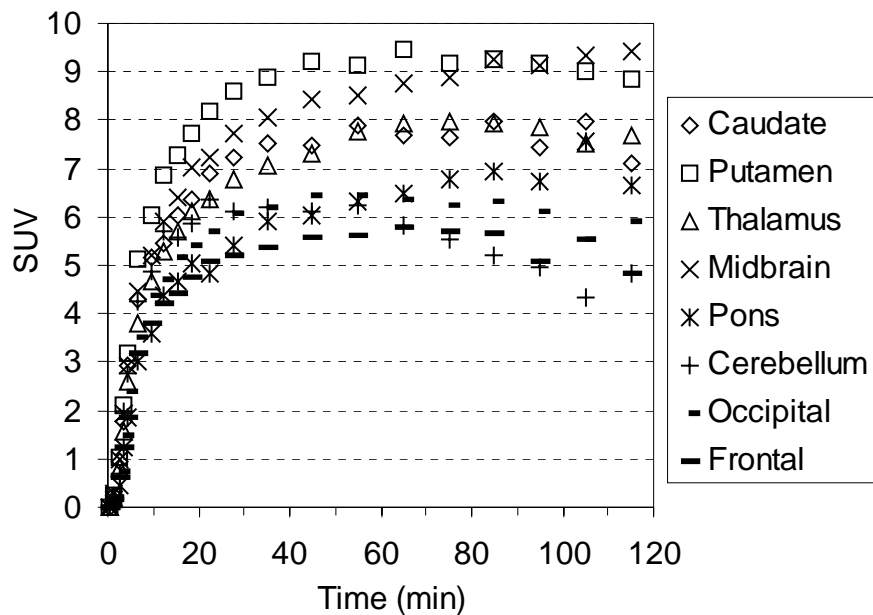


Figure S1. MicroPET baseline study TACs for the brain regions of a cynomolgus monkey after injection of $[^{11}\text{C}]1$.

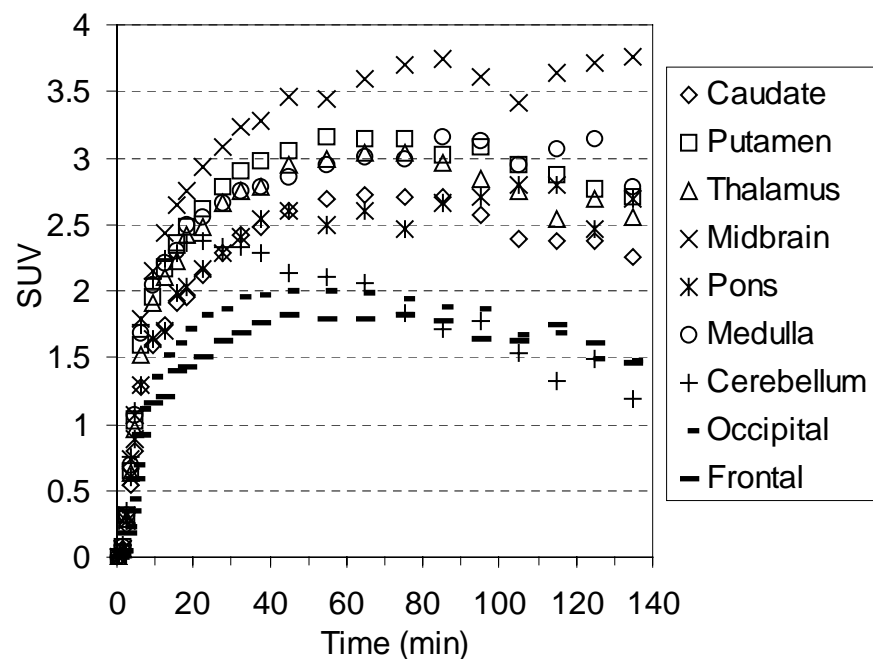


Figure S2. MicroPET baseline study TACs for the brain regions of a cynomolgus monkey after injection of $[^{11}\text{C}]2$.

Table S1. Standard uptake values (SUV) of [¹¹C]1 used to generate the TACs in Figure 1.

Time (min)	Caudate	Putamen	Thalamus	Midbrain	Pons	Medulla	Cerebellum	Occipital	Frontal
0.5	0.01	0.01	0.01	0.01	0.01	0.02	0.01	0.01	0.01
1.5	0.28	0.35	0.33	0.35	0.29	0.39	0.38	0.24	0.17
2.5	0.89	1.14	1.10	1.26	1.01	1.40	1.20	0.85	0.66
3.5	1.57	2.12	2.10	2.29	1.79	2.62	2.19	1.70	1.21
4.5	2.44	3.12	3.09	3.47	2.65	3.90	3.23	2.44	1.91
6.5	3.54	4.68	4.52	4.97	4.07	5.28	4.84	3.59	2.82
9.5	4.12	5.39	5.29	5.71	4.69	6.22	5.33	4.26	3.33
12.5	4.63	5.90	5.78	6.15	5.08	6.53	5.62	4.52	3.58
15.5	4.80	6.17	6.04	6.42	5.23	6.72	5.73	4.69	3.69
18.5	5.07	6.55	6.41	6.72	5.52	6.77	5.74	4.80	3.85
22.5	5.30	6.77	6.60	6.94	5.72	6.95	5.75	5.01	4.03
27.5	5.41	6.94	6.87	7.14	5.94	7.04	5.69	5.03	4.09
35.0	5.74	7.20	6.96	7.49	5.96	7.36	5.42	4.93	4.13
45.0	5.77	7.16	7.14	7.66	6.02	7.21	5.11	4.79	4.13
55.0	5.74	7.17	7.12	7.57	6.13	7.26	4.71	4.58	4.06
65.0	5.79	7.06	6.90	7.56	5.99	6.94	4.37	4.40	3.90
75.0	5.71	6.92	6.93	7.48	5.92	6.90	4.04	4.20	3.73
85.0	5.53	6.58	6.65	7.47	5.86	6.72	3.72	4.00	3.69
95.0	5.44	6.41	6.46	7.11	5.84	6.85	3.46	3.72	3.58
105.0	5.13	6.32	6.30	7.34	5.37	6.25	3.05	3.62	3.42
115.0	4.84	6.28	6.16	7.23	5.45	6.11	3.05	3.53	3.28

Table S2. Standard uptake values (SUV) of [¹¹C]2 used to generate the TACs in Figure 2.

Time (min)	Caudate	Putamen	Thalamus	Midbrain	Pons	Medulla	Cerebellum	Occipital	Frontal
0.5	0.01	0.01	0.01	0.01	0.01	0.02	0.01	0.01	0.01
1.5	0.24	0.30	0.27	0.33	0.34	0.40	0.35	0.20	0.17
2.5	0.73	1.01	0.83	1.11	1.09	1.32	1.10	0.65	0.57
3.5	1.57	1.96	1.54	2.19	2.09	2.50	2.13	1.34	1.07
4.5	2.33	2.94	2.40	3.29	2.99	3.57	3.48	2.14	1.57
6.5	3.67	4.44	3.58	4.84	4.43	5.27	4.91	3.25	2.33
9.5	4.35	5.41	4.30	5.59	5.30	5.99	5.57	3.70	2.85
12.5	4.60	5.62	4.57	5.89	5.57	6.27	6.13	4.08	3.04
15.5	5.21	6.07	4.87	6.32	5.76	6.52	6.06	4.55	3.21
18.5	5.43	6.37	5.21	6.73	6.46	6.74	6.13	4.55	3.37
22.5	5.56	6.52	5.34	6.80	6.34	6.96	6.05	4.82	3.47
27.5	5.98	6.85	5.55	7.01	6.51	7.08	6.18	4.92	3.61
35.0	6.21	7.00	5.87	7.40	6.84	7.19	5.92	5.12	3.70
45.0	6.63	7.28	6.07	7.58	6.91	7.17	5.58	5.27	3.76
55.0	6.73	7.38	6.40	7.74	7.56	7.31	5.35	5.30	3.82
65.0	6.90	7.28	6.39	7.92	7.50	7.11	5.01	5.14	3.80
75.0	6.61	7.45	6.31	7.93	7.27	7.18	4.79	5.07	3.78
85.0	6.78	7.16	6.55	7.92	7.24	7.01	4.50	5.21	3.83
95.0	7.04	7.42	6.34	7.89	8.08	6.80	4.09	5.20	3.85
105.0	6.76	7.17	6.47	7.72	7.11	6.81	4.02	4.78	3.70
115.0	6.42	7.10	6.26	7.72	7.58	6.59	3.76	4.66	3.54
125.0	5.66	6.69	6.09	7.81	6.47	6.20	3.74	4.40	3.65
135.0	6.18	6.51	5.83	7.82	7.40	6.29	3.49	4.33	3.43

Table S3. Comparison of the Ratio of Uptake of [¹¹C]1 and [¹¹C]2 in Specific Brain Regions to Cerebellum Uptake at 65, 85, and 105 min Post-Injection for the Baseline Studies Shown in Figures S1 and S2.

Brain Region	65 min		85 min		105 min	
	[¹¹ C]1	[¹¹ C]2	[¹¹ C]1	[¹¹ C]2	[¹¹ C]1	[¹¹ C]2
Caudate	1.3	1.3	1.5	1.6	1.8	1.6
Putamen	1.6	1.5	1.8	1.8	2.1	1.9
Thalamus	1.4	1.5	1.5	1.7	1.7	1.8
Midbrain	1.5	1.8	1.8	2.2	2.2	2.2
Pons	1.1	1.3	1.3	1.6	1.7	1.8
Medulla	N/A	1.5	N/A	1.8	N/A	1.9
Frontal	1.0	0.9	1.1	1.0	1.3	1.1
Occipital	1.1	1.0	1.2	1.1	1.3	1.1

Discussion of purity of **1** and **2**

The elemental analysis results and analytical HPLC purity for the samples of **1** and **2** used for the *in vitro* competition binding assays are shown in Table S4. The ^1H NMR spectra for **1** (Figure S3) and **2** (Figure S4) show that each sample contained residual solvent and/or grease (see Gottlieb, H. E., *et al.* *J. Org. Chem.* **1997**, *62*, 7512-7515). These minor impurities are the cause of the discrepancies observed in the elemental analysis relative to the theoretical values. The ^1H NMR spectra in Figures S3 and S4 indicate that there are both identical and nonidentical impurities in each sample. The binding data in Table 1 indicate that **1** and **2** have the same affinity for the SERT which would suggest that these impurities did not adversely affect the determination of the binding affinities.

Table S4. Elemental analysis results and HPLC purity for the samples of **1** and **2** used for the *in vitro* competition binding assays.

compd	Theory			Found ^a			HPLC (254 nm)	
	C	H	N	C	H	N	Solvent-1 ^b	Solvent-2 ^c
1	51.40	5.07	3.53	50.49	5.07	3.31	97%	99%
2	58.30	5.76	4.00	55.45	5.86	3.65	96%	86% ^d

a) Analysis performed in duplicate (average values shown) by Atlantic Microlab, Inc.

b) HPLC System 1: Waters Nova-Pak C₁₈ 3.9 x 150 mm, 75:25:0.1 v/v/v MeOH/H₂O/NEt₃, 1 mL/min.

c) HPLC System 2: Waters Xterra Prep RP₁₈ 5μm, 19 x 100 mm, 60:40:0.1 v/v/v MeOH/H₂O/NEt₃, 9.8 mL/min.

d) Sample partially decomposed upon storage – The solution of **2** in MeOH that was used for analysis with solvent system-1 was stored in the freezer for 6 months prior to analysis with solvent system-2. Elemental analysis had consumed all of the sample of **2** prior to the request during the review process that purity in a second solvent system be determined.

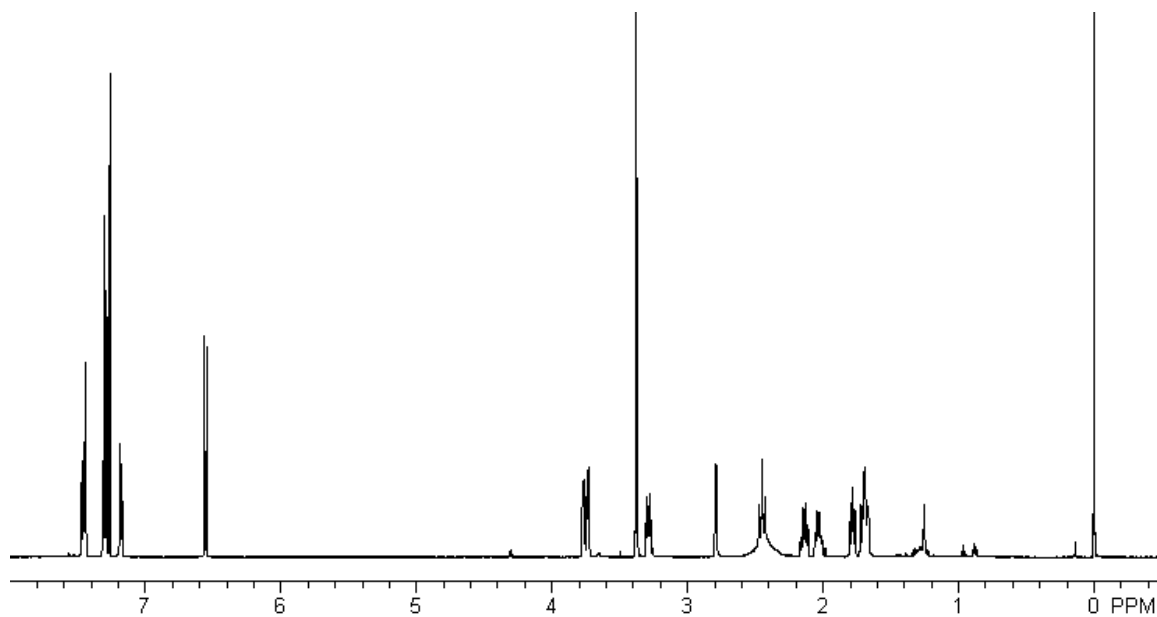


Figure S3. ¹H NMR (600 MHz, CDCl₃) Spectrum of the Sample of **1** That Was Used For the *In Vitro* Competition Binding Assays.

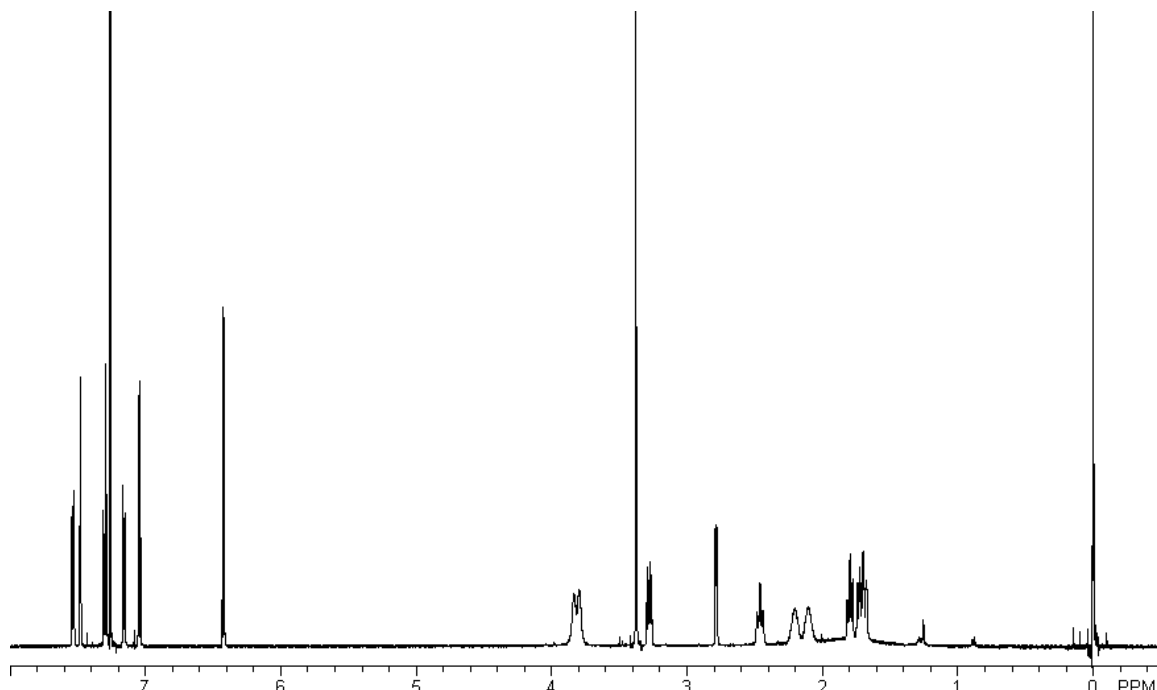


Figure S4. ¹H NMR (600 MHz, CDCl₃) Spectrum of the Sample of **2** That Was Used For the *In Vitro* Competition Binding Assays.

X-ray Crystallography

The X-ray crystal structure of **1**¹ is shown in Figures S5 and S6. Analysis of the crystal structure with Mercury 1.3 revealed several nonbonded interactions (Figure S7). Intramolecular interactions include a hydrogen bond between the carbonyl oxygen and the nitrogen proton² with a distance of 2.32 Å, and a CH-π interaction^{3,4} between the methyl ester and the phenyl ring with a proton to π-centroid distance of 3.82 Å. Intermolecular interactions include a C-H···O hydrogen bond⁵⁻⁷ between the *meta*-proton of the phenyl ring and the carbonyl oxygen atom with a distance of 2.51 Å, and a halogen bond⁸⁻¹⁰ between the iodine atom and the nitrogen lone pair with a distance of 3.10 Å. All of these types of interactions are known to be employed in biological molecular recognition^{5,9,11,12} but which of them, if any, contribute to the binding of **1** to the SERT¹³⁻¹⁷ is unknown at this time.

References

- (1) Cambridge Crystallographic Data Centre deposition number CCDC 287981
- (2) Taylor, R.; Kennard, O. Hydrogen-Bond Geometry in Organic Crystals. *Acc. Chem. Res.* **1984**, *17*, 320-326.
- (3) Kim, E.; Paliwal, S.; Wilcox, C. S. Measurements of Molecular Electrostatic Field Effects in Edge-to-Face Aromatic Interactions and CH-π Interactions with Implications for Protein Folding and Molecular Recognition. *J. Am. Chem. Soc.* **1998**, *120*, 11192-11193.
- (4) Tsue, H.; Ishibashi, K.; Takahashi, H.; Tamura, R. Exhaustively Methylated Azacalix[4]arene: Preparation, Conformation, and Crystal Structure with Exclusively CH/π-Controlled Crystal Architecture. *Org. Lett.* **2005**, *7*, 2165-2168.
- (5) Thomas, K. A.; Smith, G. M.; Thomas, T. B.; Feldmann, R. J. Electronic Distributions Within Protein Phenylalanine Aromatic Rings Are Reflected by the Three-Dimensional Oxygen Atom Environments. *Proc. Natl. Acad. Sci. USA* **1982**, *79*, 4843-4847.
- (6) Desiraju, G. R. The C-H···O Hydrogen Bond: Structural Implications and Supramolecular Design. *Acc. Chem. Res.* **1996**, *29*, 441-449.
- (7) Steiner, T.; Desiraju, G. R. Distinction between the weak hydrogen bond and the van der Waals interaction. *Chem. Commun.* **1998**, 891-892.
- (8) Lommerse, J. P. M.; Stone, A. J.; Taylor, R.; Allen, F. H. The Nature and Geometry of Intermolecular Interactions between Halogens and Oxygen or Nitrogen. *J. Am. Chem. Soc.* **1996**, *118*, 3108-3116.
- (9) Auffinger, P.; Hays, F. A.; Westhof, E.; Ho, P. S. Halogen Bonds in Biological Molecules. *Proc. Natl. Acad. Sci. USA* **2004**, *101*, 16789-16794.
- (10) Metrangolo, P.; Neukirch, H.; Pilati, T.; Resnati, G. Halogen Bonding Based Recognition Processes: A World Parallel to Hydrogen Bonding. *Acc. Chem. Res.* **2005**, *38*, 386-395.
- (11) Meyer, E. A.; Castellano, R. K.; Diederich, F. Interactions with Aromatic Rings in Chemical and Biological Recognition. *Angew. Chem. Int. Ed.* **2003**, *42*, 1210-1250.
- (12) Klebe, G. The Use of Composite Crystal-Field Environments in Molecular Recognition and the *de Novo* Design of Protein Ligands. *J. Mol. Biol.* **1994**, *237*, 212-235.
- (13) Ravna, A. W.; Edvardsen, Ø. A Putative Three-Dimensional Arrangement of the Human Serotonin Transporter Transmembrane Helices: A Tool to Aid Experimental Studies. *J. Mol. Graph. Model.* **2001**, *20*, 133-144.
- (14) Ravna, A. W.; Sylte, I.; Kristiansen, K.; Dahl, S. G. Putative Drug Binding Conformations of Monoamine Transporters. *Bioorg. Med. Chem.* **2006**, *14*, 666-675.

- (15) Ravna, A. W.; Sylte, I.; Dahl, S. G. Molecular Mechanism of Citalopram and Cocaine Interactions with Neurotransmitter Transporters. *J. Pharm. Exp. Ther.* **2003**, *307*, 34-41.
- (16) Roman, D. L.; Saldaña, S. N.; Nichols, D. E.; Carroll, F. I.; Barker, E. L. Distinct Molecular Recognition of Psychostimulants by Human and *Drosophila* Serotonin Transporters. *J. Pharm. Exp. Ther.* **2004**, *308*, 679-687.
- (17) Muszynski, I. C.; Scapozza, L.; Kovar, K.-A.; Folkers, G. Quantitative Structure-Activity Relationships of Phenyltropanes as Inhibitors of Three Monoamine Transporters: Classical and CoMFA studies. *Quant. Struct.-Act. Relat.* **1999**, *18*, 342-353.

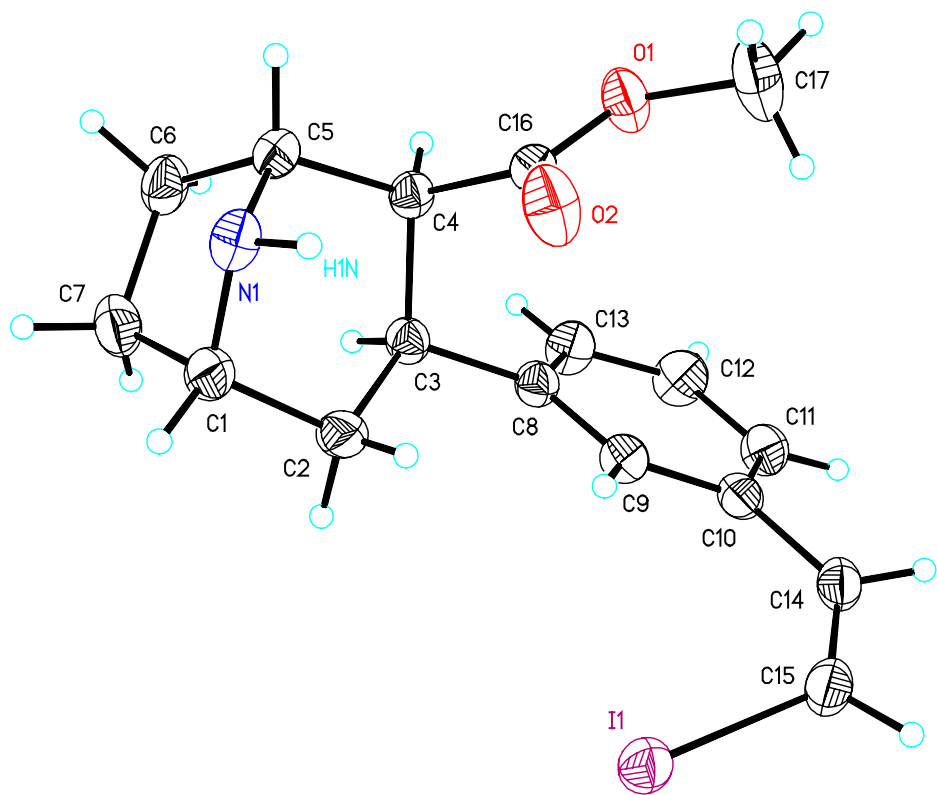


Figure S5. Thermal ellipsoid representation of the X-ray crystal structure of **1**.

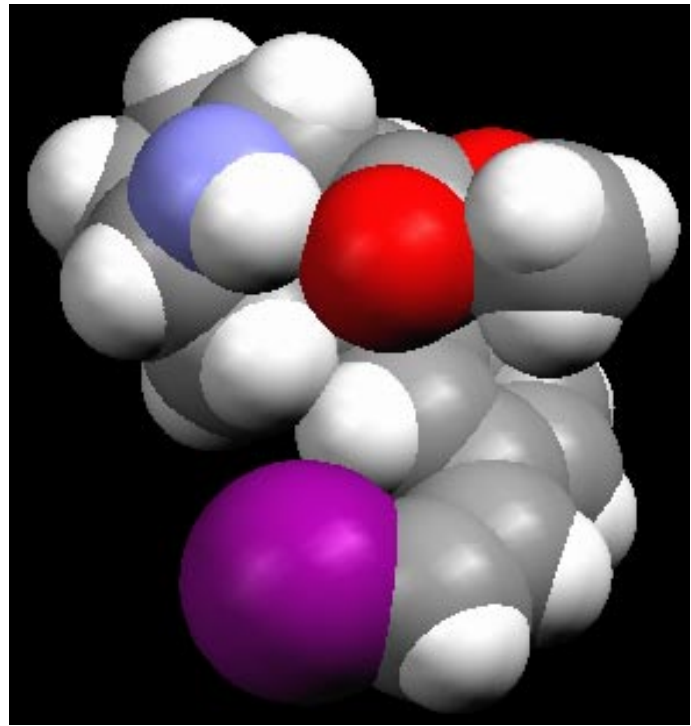


Figure S6. Space filling representation of the X-ray crystal structure of **1**.

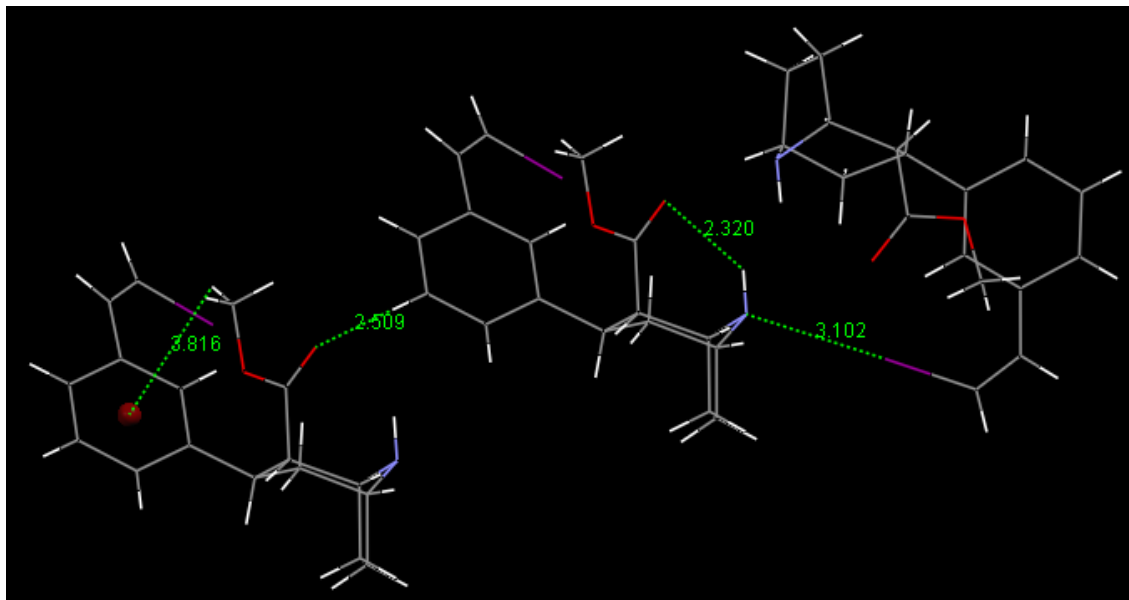


Figure S7. Measured distances (\AA) of several nonbonded interactions in the X-ray crystal structure of **1**.

Crystallography Experimental

A suitable crystal of **1** was coated with Paratone N oil, suspended in a small fiber loop and placed in a cooled nitrogen gas stream at 173 K on a Bruker D8 SMART APEX CCD sealed tube diffractometer with graphite monochromated MoK α (0.71073 Å) radiation. Data were measured using a series of combinations of phi and omega scans with 10 s frame exposures and 0.3° frame widths. Data collection, indexing and initial cell refinements were all carried out using SMART¹ software. Frame integration and final cell refinements were done using SAINT² software. The final cell parameters were determined from least-squares refinement on 7356 reflections. The SADABS³ program was used to carry out absorption corrections.

The structure was solved using Direct methods and difference Fourier techniques (SHELXTL, V6.12).⁴ Hydrogen atoms were placed their expected chemical positions using the HFIX command and were included in the final cycles of least squares with isotropic U_{ij} 's related to the atom's ridden upon. The C-H distances were fixed at 0.93 Å(aromatic and amide), 0.98 Å (methine), 0.97 Å (methylene), or 0.96 Å (methyl). All non-hydrogen atoms were refined anisotropically. Scattering factors and anomalous dispersion corrections are taken from the *International Tables for X-ray Crystallography*⁵. Structure solution, refinement, graphics and generation of publication materials were performed by using SHELXTL, V6.12 software. Additional details of data collection and structure refinement are given in Table S5.

References

1. SMART Version 5.628, **2003**, Bruker AXS, Inc., Analytical X-ray Systems, 5465 East Cheryl Parkway, Madison WI 53711-5373.
2. SAINT Version 6.36A, **2002**, Bruker AXS, Inc., Analytical X-ray Systems, 5465 East Cheryl Parkway, Madison WI 53711-5373.
3. SADABS Version 2.10, **2003**, George Sheldrick, University of Göttingen,
4. SHELXTL V6.12, **2002**, Bruker AXS, Inc., Analytical X-ray Systems, 5465 East Cheryl Parkway, Madison WI 53711-5373.
5. A. J. C. Wilson (ed), *International Tables for X-ray Crystallography, Volume C*. Kynoch, Academic Publishers, Dordrecht, **1992**, Tables 6.1.1.4 (pp. 500-502) and 4.2.6.8 (pp. 219-222).

Table S5. Crystal data and structure refinement for **1**.

Identification code	<i>mZIENT, 1</i>
Empirical formula	C17 H20 I N O2
Formula weight	397.24
Temperature	173(2) K
Wavelength	0.71073 Å
Crystal system	Orthorhombic
Space group	P2(1)2(1)2(1)
Unit cell dimensions	a = 8.0624(5) Å α = 90°. b = 10.8200(7) Å β = 90°. c = 18.7082(12) Å γ = 90°.
Volume	1632.01(18) Å ³
Z	4
Density (calculated)	1.617 Mg/m ³
Absorption coefficient	1.966 mm ⁻¹
F(000)	792
Crystal size	0.33 x 0.30 x 0.20 mm ³
Theta range for data collection	2.17 to 28.30°.
Index ranges	-10<=h<=10, -14<=k<=14, -24<=l<=24
Reflections collected	22649
Independent reflections	4037 [R(int) = 0.0232]
Completeness to theta = 28.31°	99.9 %
Absorption correction	Semi-empirical from equivalents
Max. and min. transmission	0.6945 and 0.5631
Refinement method	Full-matrix least-squares on F ²
Data / restraints / parameters	4037 / 0 / 191
Goodness-of-fit on F ²	1.009
Final R indices [I>2sigma(I)]	R1 = 0.0186, wR2 = 0.0500
R indices (all data)	R1 = 0.0191, wR2 = 0.0503
Absolute structure parameter	-0.025(14)
Largest diff. peak and hole	0.644 and -0.249 e.Å ⁻³

Table S6. Atomic coordinates ($\times 10^4$) and equivalent isotropic displacement parameters ($\text{\AA}^2 \times 10^3$) for **1**. U(eq) is defined as one third of the trace of the orthogonalized U^{ij} tensor.

	x	y	z	U(eq)
I(1)	2834(1)	4485(1)	782(1)	32(1)
C(1)	3907(3)	7261(2)	3289(1)	30(1)
C(2)	2669(3)	6862(2)	2715(1)	31(1)
C(3)	1201(2)	7763(2)	2659(1)	23(1)
C(4)	1793(2)	9138(2)	2675(1)	23(1)
C(5)	3173(2)	9309(2)	3241(1)	26(1)
C(6)	2555(3)	8871(2)	3977(1)	32(1)
C(7)	3089(3)	7506(2)	4018(1)	35(1)
C(8)	43(2)	7523(2)	2036(1)	24(1)
C(9)	601(2)	6989(2)	1402(1)	25(1)
C(10)	-471(2)	6772(2)	829(1)	25(1)
C(11)	-2107(3)	7175(2)	882(1)	31(1)
C(12)	-2674(3)	7729(2)	1510(1)	37(1)
C(13)	-1619(3)	7877(2)	2086(1)	32(1)
C(14)	44(3)	6157(2)	164(1)	28(1)
C(15)	1212(3)	5314(2)	43(1)	31(1)
C(16)	2351(2)	9542(2)	1940(1)	25(1)
C(17)	1604(4)	10646(3)	906(1)	48(1)
N(1)	4596(2)	8489(2)	3127(1)	29(1)
O(1)	1259(2)	10313(2)	1637(1)	35(1)
O(2)	3596(2)	9217(2)	1644(1)	39(1)

Table S7. Bond lengths [\AA] and angles [$^\circ$] for **1**.

I(1)-C(15)	2.103(2)	C(14)-H(14)	0.9300
C(1)-N(1)	1.472(3)	C(15)-H(15)	0.9300
C(1)-C(2)	1.527(3)	C(16)-O(2)	1.199(3)
C(1)-C(7)	1.539(3)	C(16)-O(1)	1.339(2)
C(1)-H(1)	0.9800	C(17)-O(1)	1.443(2)
C(2)-C(3)	1.537(3)	C(17)-H(17A)	0.9600
C(2)-H(2A)	0.9700	C(17)-H(17B)	0.9600
C(2)-H(2B)	0.9700	C(17)-H(17C)	0.9600
C(3)-C(8)	1.517(3)	N(1)-H(1N)	0.9231
C(3)-C(4)	1.563(2)		
C(3)-H(3)	0.9800	N(1)-C(1)-C(2)	110.91(17)
C(4)-C(16)	1.512(2)	N(1)-C(1)-C(7)	100.85(16)
C(4)-C(5)	1.547(3)	C(2)-C(1)-C(7)	113.06(18)
C(4)-H(4)	0.9800	N(1)-C(1)-H(1)	110.6
C(5)-N(1)	1.466(3)	C(2)-C(1)-H(1)	110.6
C(5)-C(6)	1.540(3)	C(7)-C(1)-H(1)	110.6
C(5)-H(5)	0.9800	C(1)-C(2)-C(3)	111.86(16)
C(6)-C(7)	1.541(3)	C(1)-C(2)-H(2A)	109.2
C(6)-H(6A)	0.9700	C(3)-C(2)-H(2A)	109.2
C(6)-H(6B)	0.9700	C(1)-C(2)-H(2B)	109.2
C(7)-H(7A)	0.9700	C(3)-C(2)-H(2B)	109.2
C(7)-H(7B)	0.9700	H(2A)-C(2)-H(2B)	107.9
C(8)-C(9)	1.393(3)	C(8)-C(3)-C(2)	114.71(16)
C(8)-C(13)	1.397(3)	C(8)-C(3)-C(4)	111.46(15)
C(9)-C(10)	1.397(3)	C(2)-C(3)-C(4)	111.56(15)
C(9)-H(9)	0.9300	C(8)-C(3)-H(3)	106.1
C(10)-C(11)	1.392(3)	C(2)-C(3)-H(3)	106.1
C(10)-C(14)	1.471(3)	C(4)-C(3)-H(3)	106.1
C(11)-C(12)	1.395(3)	C(16)-C(4)-C(5)	111.95(15)
C(11)-H(11)	0.9300	C(16)-C(4)-C(3)	110.37(15)
C(12)-C(13)	1.382(3)	C(5)-C(4)-C(3)	110.29(15)
C(12)-H(12)	0.9300	C(16)-C(4)-H(4)	108.0
C(13)-H(13)	0.9300	C(5)-C(4)-H(4)	108.0
C(14)-C(15)	1.331(3)	C(3)-C(4)-H(4)	108.0

N(1)-C(5)-C(6)	101.39(15)	C(15)-C(14)-C(10)	130.84(18)
N(1)-C(5)-C(4)	113.00(15)	C(15)-C(14)-H(14)	114.6
C(6)-C(5)-C(4)	110.02(16)	C(10)-C(14)-H(14)	114.6
N(1)-C(5)-H(5)	110.7	C(14)-C(15)-I(1)	128.34(15)
C(6)-C(5)-H(5)	110.7	C(14)-C(15)-H(15)	115.8
C(4)-C(5)-H(5)	110.7	I(1)-C(15)-H(15)	115.8
C(5)-C(6)-C(7)	104.43(16)	O(2)-C(16)-O(1)	122.55(18)
C(5)-C(6)-H(6A)	110.9	O(2)-C(16)-C(4)	125.80(18)
C(7)-C(6)-H(6A)	110.9	O(1)-C(16)-C(4)	111.64(16)
C(5)-C(6)-H(6B)	110.9	O(1)-C(17)-H(17A)	109.5
C(7)-C(6)-H(6B)	110.9	O(1)-C(17)-H(17B)	109.5
H(6A)-C(6)-H(6B)	108.9	H(17A)-C(17)-H(17B)	109.5
C(1)-C(7)-C(6)	103.94(16)	O(1)-C(17)-H(17C)	109.5
C(1)-C(7)-H(7A)	111.0	H(17A)-C(17)-H(17C)	109.5
C(6)-C(7)-H(7A)	111.0	H(17B)-C(17)-H(17C)	109.5
C(1)-C(7)-H(7B)	111.0	C(5)-N(1)-C(1)	102.80(15)
C(6)-C(7)-H(7B)	111.0	C(5)-N(1)-H(1N)	110.6
H(7A)-C(7)-H(7B)	109.0	C(1)-N(1)-H(1N)	112.4
C(9)-C(8)-C(13)	118.71(18)	C(16)-O(1)-C(17)	115.44(17)
C(9)-C(8)-C(3)	121.79(17)		
C(13)-C(8)-C(3)	119.47(17)		
C(8)-C(9)-C(10)	121.52(18)		
C(8)-C(9)-H(9)	119.2		
C(10)-C(9)-H(9)	119.2		
C(11)-C(10)-C(9)	118.61(18)		
C(11)-C(10)-C(14)	117.98(18)		
C(9)-C(10)-C(14)	123.39(17)		
C(10)-C(11)-C(12)	120.3(2)		
C(10)-C(11)-H(11)	119.8		
C(12)-C(11)-H(11)	119.8		
C(13)-C(12)-C(11)	120.3(2)		
C(13)-C(12)-H(12)	119.9		
C(11)-C(12)-H(12)	119.9		
C(12)-C(13)-C(8)	120.42(19)		
C(12)-C(13)-H(13)	119.8		
C(8)-C(13)-H(13)	119.8		

Symmetry transformations used to generate equivalent atoms:

Table S8. Anisotropic displacement parameters ($\text{\AA}^2 \times 10^3$) for **1**. The anisotropic displacement factor exponent takes the form: $-2\pi^2 [h^2 a^{*2} U^{11} + \dots + 2 h k a^{*} b^{*} U^{12}]$

	U ¹¹	U ²²	U ³³	U ²³	U ¹³	U ¹²
I(1)	34(1)	34(1)	28(1)	-3(1)	-1(1)	7(1)
C(1)	30(1)	29(1)	31(1)	-3(1)	-8(1)	6(1)
C(2)	32(1)	24(1)	35(1)	-3(1)	-10(1)	6(1)
C(3)	22(1)	25(1)	24(1)	1(1)	-2(1)	2(1)
C(4)	24(1)	25(1)	20(1)	-2(1)	2(1)	4(1)
C(5)	31(1)	26(1)	22(1)	-3(1)	-2(1)	1(1)
C(6)	36(1)	40(1)	21(1)	-4(1)	0(1)	5(1)
C(7)	38(1)	40(1)	28(1)	8(1)	-5(1)	-1(1)
C(8)	24(1)	24(1)	24(1)	1(1)	-2(1)	0(1)
C(9)	21(1)	27(1)	27(1)	1(1)	0(1)	1(1)
C(10)	26(1)	23(1)	26(1)	3(1)	-2(1)	0(1)
C(11)	27(1)	33(1)	33(1)	0(1)	-8(1)	5(1)
C(12)	25(1)	43(1)	43(1)	-5(1)	-5(1)	10(1)
C(13)	26(1)	39(1)	30(1)	-3(1)	0(1)	6(1)
C(14)	32(1)	30(1)	23(1)	3(1)	-4(1)	-4(1)
C(15)	36(1)	35(1)	22(1)	-1(1)	-1(1)	-2(1)
C(16)	27(1)	24(1)	23(1)	0(1)	-3(1)	-2(1)
C(17)	53(1)	64(2)	28(1)	16(1)	4(1)	17(1)
N(1)	25(1)	38(1)	24(1)	-3(1)	-1(1)	1(1)
O(1)	40(1)	40(1)	25(1)	7(1)	1(1)	14(1)
O(2)	29(1)	58(1)	30(1)	11(1)	9(1)	12(1)

Table S9. Hydrogen coordinates ($\times 10^4$) and isotropic displacement parameters ($\text{\AA}^2 \times 10^{-3}$) for **1**.

	x	y	z	U(eq)
H(1)	4798	6650	3335	36
H(2A)	2256	6043	2828	37
H(2B)	3230	6818	2257	37
H(3)	539	7641	3093	28
H(4)	847	9654	2815	27
H(5)	3531	10174	3262	32
H(6A)	1359	8948	4012	39
H(6B)	3062	9349	4358	39
H(7A)	3872	7376	4405	42
H(7B)	2138	6971	4090	42
H(9)	1713	6772	1359	30
H(11)	-2825	7074	498	37
H(12)	-3766	7999	1541	44
H(13)	-2018	8215	2509	38
H(14)	-546	6398	-240	34
H(15)	1326	5058	-429	37
H(17A)	2708	10975	872	73
H(17B)	822	11258	750	73
H(17C)	1514	9926	608	73
H(1N)	4973	8549	2662	35

Table S10. Torsion angles [°] for **1**.

N(1)-C(1)-C(2)-C(3)	-60.3(2)
C(7)-C(1)-C(2)-C(3)	52.1(2)
C(1)-C(2)-C(3)-C(8)	172.16(17)
C(1)-C(2)-C(3)-C(4)	44.2(2)
C(8)-C(3)-C(4)-C(16)	-47.04(19)
C(2)-C(3)-C(4)-C(16)	82.63(19)
C(8)-C(3)-C(4)-C(5)	-171.26(15)
C(2)-C(3)-C(4)-C(5)	-41.6(2)
C(16)-C(4)-C(5)-N(1)	-66.8(2)
C(3)-C(4)-C(5)-N(1)	56.6(2)
C(16)-C(4)-C(5)-C(6)	-179.28(15)
C(3)-C(4)-C(5)-C(6)	-56.0(2)
N(1)-C(5)-C(6)-C(7)	-27.62(19)
C(4)-C(5)-C(6)-C(7)	92.22(19)
N(1)-C(1)-C(7)-C(6)	31.12(19)
C(2)-C(1)-C(7)-C(6)	-87.3(2)
C(5)-C(6)-C(7)-C(1)	-2.2(2)
C(2)-C(3)-C(8)-C(9)	-29.3(3)
C(4)-C(3)-C(8)-C(9)	98.7(2)
C(2)-C(3)-C(8)-C(13)	152.67(19)
C(4)-C(3)-C(8)-C(13)	-79.3(2)
C(13)-C(8)-C(9)-C(10)	-1.8(3)
C(3)-C(8)-C(9)-C(10)	-179.89(17)
C(8)-C(9)-C(10)-C(11)	4.2(3)
C(8)-C(9)-C(10)-C(14)	-176.93(18)
C(9)-C(10)-C(11)-C(12)	-3.1(3)
C(14)-C(10)-C(11)-C(12)	177.97(19)
C(10)-C(11)-C(12)-C(13)	-0.3(3)
C(11)-C(12)-C(13)-C(8)	2.7(4)
C(9)-C(8)-C(13)-C(12)	-1.6(3)
C(3)-C(8)-C(13)-C(12)	176.5(2)
C(11)-C(10)-C(14)-C(15)	-152.0(2)
C(9)-C(10)-C(14)-C(15)	29.0(3)
C(10)-C(14)-C(15)-I(1)	0.5(3)

C(5)-C(4)-C(16)-O(2)	51.4(3)
C(3)-C(4)-C(16)-O(2)	-71.9(2)
C(5)-C(4)-C(16)-O(1)	-129.64(17)
C(3)-C(4)-C(16)-O(1)	107.09(18)
C(6)-C(5)-N(1)-C(1)	48.95(18)
C(4)-C(5)-N(1)-C(1)	-68.76(19)
C(2)-C(1)-N(1)-C(5)	69.63(19)
C(7)-C(1)-N(1)-C(5)	-50.39(17)
O(2)-C(16)-O(1)-C(17)	5.1(3)
C(4)-C(16)-O(1)-C(17)	-173.87(19)

Symmetry transformations used to generate equivalent atoms:

Table S11. Hydrogen bonds for **1** [Å and °].

D-H...A	d(D-H)	d(H...A)	d(D...A)	<(DHA)
N(1)-H(1N)...O(2)	0.92	2.32	2.994(2)	129.6

Symmetry transformations used to generate equivalent atoms: